

IMPLICATIONS OF MASS AND ENERGY LOSS DUE TO CORONAL MASS EJECTIONS ON MAGNETICALLY ACTIVE STARS

JEREMY J. DRAKE¹, OFER COHEN¹, SEIJI YASHIRO^{2,3}, AND NAT GOPALSWAMY³

¹ Harvard-Smithsonian Center for Astrophysics, 60 Garden Street, Cambridge, MA 02138, USA; jdrake@cfa.harvard.edu

² Interferometrics Inc., Herndon, VA 20171, USA

³ NASA Goddard Space Flight Center, Greenbelt, MD 20771, USA

Received 2012 July 27; accepted 2013 January 12; published 2013 February 5

ABSTRACT

Analysis of a database of solar coronal mass ejections (CMEs) and associated flares over the period 1996–2007 finds well-behaved power-law relationships between the 1–8 Å flare X-ray fluence and CME mass and kinetic energy. We extrapolate these relationships to lower and higher flare energies to estimate the mass and energy loss due to CMEs from stellar coronae, assuming that the observed X-ray emission of the latter is dominated by flares with a frequency as a function of energy $dn/dE = kE^{-\alpha}$. For solar-like stars at saturated levels of X-ray activity, the implied losses depend fairly weakly on the assumed value of α and are very large: $\dot{M} \sim 5 \times 10^{-10} M_{\odot} \text{ yr}^{-1}$ and $\dot{E} \sim 0.1 L_{\odot}$. In order to avoid such large energy requirements, either the relationships between CME mass and speed and flare energy must flatten for X-ray fluence $\gtrsim 10^{31}$ erg, or the flare–CME association must drop significantly below 1 for more energetic events. If active coronae are dominated by flares, then the total coronal energy budget is likely to be up to an order of magnitude larger than the canonical $10^{-3} L_{\text{bol}}$ X-ray saturation threshold. This raises the question of what is the maximum energy a magnetic dynamo can extract from a star? For an energy budget of 1% of L_{bol} , the CME mass loss rate is about $5 \times 10^{-11} M_{\odot} \text{ yr}^{-1}$.

Key words: stars: flare – stars: winds, outflows – Sun: coronal mass ejections (CMEs) – X-rays: stars

Online-only material: color figures

1. INTRODUCTION

The rate of mass loss from unevolved late-type stars is notoriously difficult to constrain. In case of the Sun, the wind can be directly observed and sampled by spacecraft, and amounts to a mass loss rate of about $2 \times 10^{-14} M_{\odot} \text{ yr}^{-1}$. Such a weak flow of ionized gas from other stars cannot be detected directly using instrumentation available today, and there are presently no *direct* detections or measurements of winds from solar-like stars. Mass loss rate upper limits based on radio observations are in the range of several $10^{-11} M_{\odot} \text{ yr}^{-1}$ (e.g., Gaidos et al. 2000). Wood et al. (2002) devised a method of indirect assessment based on H Ly α absorption due to interstellar H I that is heated in the interaction region between the wind and the local interstellar medium. They estimated rates in the range 10^{-15} – $10^{-12} M_{\odot} \text{ yr}^{-1}$, with evidence for higher mass loss rates for more X-ray luminous stars.

Theoretical progress in predicting solar-like winds has been hampered by a persistent lack of understanding of the basic mechanisms responsible for producing them. Inspired by the recent success of turbulence-driven coronal heating and solar wind acceleration theory, Cranmer & Saar (2011) developed a wind model based on the energy flux of magnetohydrodynamic turbulence from the subsurface convection zone. For a solar-like star, they predict mass loss rates that decline steadily from a few $10^{-12} M_{\odot} \text{ yr}^{-1}$ at the zero-age main sequence and rotation periods of 1 day to $\sim 10^{-15} M_{\odot} \text{ yr}^{-1}$ at rotation periods of 60 days or so, in reasonable agreement with the estimates of Wood et al. (2002; see also Wood et al. 2005).

Further progress in understanding mass loss of main-sequence late-type stars is strongly motivated by the effect winds have on stellar rotation evolution (e.g., Weber & Davis 1967; Stauffer & Hartmann 1986; Kawaler 1988; Matt & Pudritz 2008;

Reiners & Mohanty 2012) and consequently on stellar magnetic activity (e.g., Pallavicini et al. 1981; Wright et al. 2011), and on interplanetary medium environments (e.g., Preusse et al. 2005; Lammer et al. 2007).

One aspect of mass loss that remains to be thoroughly investigated on other late-type stars is that due to coronal mass ejections (CMEs). On the Sun, CMEs are observed to eject from 10^{13} to 10^{17} g of magnetized plasma into the interplanetary medium (e.g., Yashiro & Gopalswamy 2009; Vourlidis et al. 2010). The integrated mass loss from CMEs can amount to several percent of the steady wind rate (e.g., Vourlidis et al. 2010). At first sight this suggests that CMEs are going to be of little importance in the stellar context. However, on the Sun CMEs are associated with flares, and magnetically active stars are widely interpreted to be dominated by flares (e.g., Guedel 1997; Drake et al. 2000). Since the most magnetically active solar-like stars can attain X-ray luminosities more than 1000 times that of the Sun, there is scope for vigorous CME activity, especially in the context of recent giant flare detections on solar-type stars based on optical *Kepler* photometry by Maehara et al. (2012). The importance of CMEs on active stars has also been raised in the context of erosion of the atmospheres of “hot Jupiters” (Khodachenko et al. 2007a) and the habitability of planets around M dwarfs (Khodachenko et al. 2007b), while Aarnio et al. (2012) suggest that CMEs associated with flares could be an important contribution to angular momentum loss on pre-main-sequence stars.

Here, we examine the consequences for mass loss and energy loss of flare-dominated coronae based on extrapolation of the observed behavior of a large sample of CMEs compiled by Yashiro & Gopalswamy (2009). The implications are quite striking and provide an indirect means to begin to assess how CMEs might behave on stars much more magnetically active than the Sun.

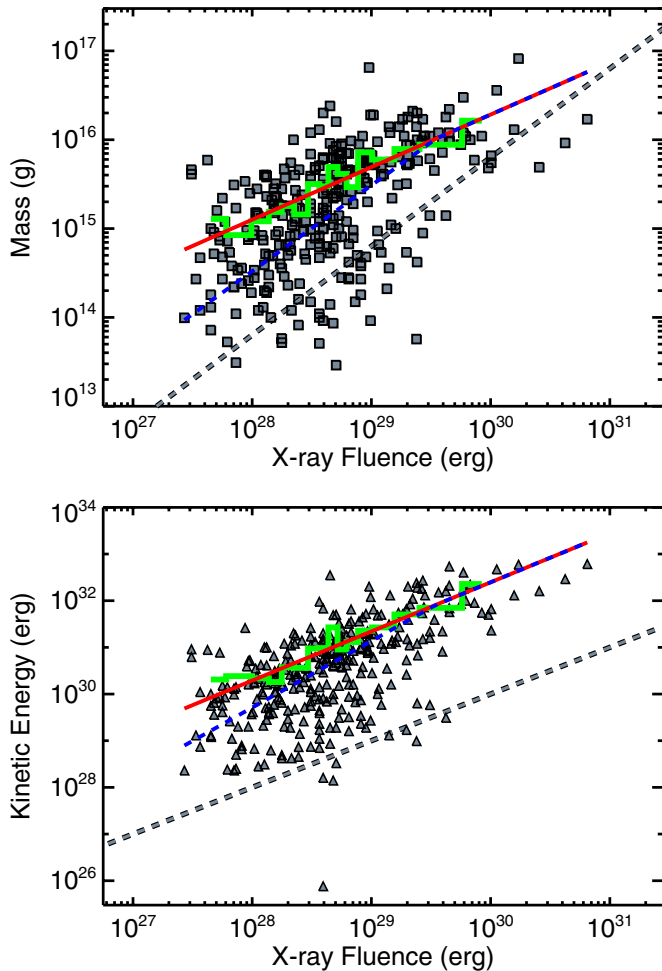


Figure 1. CME mass (top) and kinetic energy (bottom) vs. X-ray fluence of the associated flare from the Yashiro & Gopalswamy (2009) sample. The green histograms are the means over 20 data points and the red lines are linear fits to these means. The dashed blue lines are the linear fits multiplied by the CME–flare association rate given by Equation (3). In the upper panel, the dashed gray line follows a constant ratio of mass loss to *GOES* X-ray energy loss, expressed as rates, $\dot{M} = 10^{-10}(L_X/10^{30}) M_\odot \text{ yr}^{-1}$. In the lower panel, the dashed gray line represents equivalence of the kinetic and X-ray energies. The red line in this panel corresponds very closely to a factor of 200 times the X-ray fluence.

(A color version of this figure is available in the online journal.)

2. MASS AND ENERGY OF SOLAR CORONAL MASS EJECTIONS

As a guide to the CME behavior of active stars, we look to the Sun. Yashiro & Gopalswamy (2009) studied the statistical relationships between solar flares and CMEs observed over the period 1996–2007 (see also Vourlidas et al. 2010 for a description of some of the observational aspects of CME measurements). They compiled a database of soft X-ray flares observed by the *Geostationary Operational Environmental Satellite (GOES)* that were associated with CMEs observed by the Large Angle and Spectrometric Coronagraph on board the *Solar and Heliospheric Observatory* mission. The CME–flare association fraction was observed to increase with flare peak X-ray flux, fluence, and duration, as had been noted in earlier studies (e.g., Andrews 2003), and a good correlation was found between the flare fluence and the CME kinetic energy.

The distribution of CME ejected masses as a function of the associated flare *GOES* 1–8 Å X-ray fluence from the Yashiro & Gopalswamy (2009) sample is illustrated in Figure 1. While

the data show a very large scatter in CME mass at a given flare energy, we find that the mean of these data over small X-ray fluence bins is well behaved and adheres quite closely to a power law. Such a power-law relation between ejected mass and the peak X-ray flux of the associated flare has also been pointed out by Aarnio et al. (2011). A linear fit to the logarithm of the variance-weighted means of 20 point bins yields the following power-law relationship (in cgs units) between ejected mass and flare fluence,

$$m_c(E) = \mu E^\beta;$$

$$\mu = 10^{-1.5 \pm 0.5}, \quad \beta = 0.59 \pm 0.02. \quad (1)$$

The constant of proportionality and power-law index uncertainties are strongly anti-correlated. They were determined using a Monte Carlo multiple imputation bootstrap (Rubin 1996) in which the distribution of fit parameters was estimated from repeated re-fitting of a randomly drawn two-thirds of the data augmented to the full sample size by random draws from this sub-sample.

Yashiro & Gopalswamy (2009) found a similar distribution of CME kinetic energy as a function of associated flare X-ray fluence. The data are shown in Figure 1, together with the histogram of the mean of every 20 points and a power-law fit to this. From this fit we find the mean CME kinetic energy to vary with flare X-ray fluence as (again in cgs units)

$$E_{ke} = \eta E^\gamma;$$

$$\eta = 10^{0.81 \pm 0.85}, \quad \gamma = 1.05 \pm 0.03. \quad (2)$$

Again, the uncertainties were determined using a Monte Carlo multiple imputation bootstrap and are essentially anti-correlated. Also shown in Figure 1 is the locus of equivalence between X-ray and kinetic energies. The latter lies about a factor of 200 above the former, indicating that, for a given flare, the energy release will be totally dominated by the energy of the associated mass ejection. We return to the consequences of this in Section 4.

We will find it useful below to also express the CME–flare association fraction as a power law. We find the Yashiro & Gopalswamy (2009) association fraction as a function of X-ray fluence, $f(E)$, can be well represented by

$$f(E) = 1 \quad \text{for } E > 3.5 \times 10^{29} \text{ erg}$$

$$f(E) = \zeta E^\delta \quad \text{for } E \leq 3.5 \times 10^{29} \text{ erg};$$

$$\zeta = 7.9 \times 10^{-12}, \quad \delta = 0.37. \quad (3)$$

3. ESTIMATING TOTAL STELLAR CME-ASSOCIATED ENERGY AND MASS LOSS

Flare occurrence in the coronae of the Sun and stars has been shown by a number of studies to follow a power-law distribution in frequency as a function of flare energy of the form

$$\frac{dn}{dE} = k E^{-\alpha}, \quad (4)$$

where k is a normalization constant (e.g., Drake 1971; Datlowe et al. 1974; Lin et al. 1984; Hudson 1991; Bai 1993; Porter et al. 1995; Krucker & Benz 1998; Audard et al. 2000; Kashyap et al. 2002; Güdel et al. 2003; Hannah et al. 2011). Analyses of stellar EUV and X-ray light curves furthermore suggest that

active stellar coronae are dominated by a superposition of flares, and tend to find values of the frequency versus energy power-law index in the range $\alpha = 2$ – 2.5 for all stellar types, including dwarfs with spectral type G–M (Audard et al. 2000; Kashyap et al. 2002; Güdel et al. 2003; Telleschi et al. 2005; see also the earlier work of Collura et al. 1988), and T Tauri stars (Caramazza et al. 2007; Stelzer et al. 2007). Similar indices were observed for optical flares detected on solar-type stars by Maehara et al. (2012) from *Kepler* photometry.

The total flare power is given by the integral over minimum and maximum flare energies

$$P = \int_{E_{\min}}^{E_{\max}} EkE^{-\alpha} dE = \frac{k}{2-\alpha} [E_{\max}^{2-\alpha} - E_{\min}^{2-\alpha}]. \quad (5)$$

Taking the X-ray luminosity, L_X , as the observable proxy for the flare power, the constant k is given by

$$k = \frac{L_X(2-\alpha)}{(E_{\max}^{2-\alpha} - E_{\min}^{2-\alpha})}. \quad (6)$$

For the case in which CME mass loss is a function of the associated flare X-ray fluence, the total mass loss rate from CMEs is

$$\dot{M}_c = \int_{E_{\min}}^{E_{\max}} m_c(E) f(E) \frac{dn}{dE} dE. \quad (7)$$

When combined with Equations (1), (3), and (6), the resulting rate is

$$\dot{M}_c = \mu\zeta L_X \left(\frac{2-\alpha}{1+\beta+\delta-\alpha} \right) \left[\frac{E_{\max}^{1+\beta+\delta-\alpha} - E_{\min}^{1+\beta+\delta-\alpha}}{E_{\max}^{2-\alpha} - E_{\min}^{2-\alpha}} \right], \quad (8)$$

which we can now evaluate for suitable choices of the minimum and maximum flare energies. Similarly, the total CME-associated kinetic energy loss rate is

$$\dot{E}_{ke} = \eta\zeta L_X \left(\frac{2-\alpha}{1+\gamma+\delta-\alpha} \right) \left[\frac{E_{\max}^{1+\gamma+\delta-\alpha} - E_{\min}^{1+\gamma+\delta-\alpha}}{E_{\max}^{2-\alpha} - E_{\min}^{2-\alpha}} \right]. \quad (9)$$

Mass loss and kinetic energy loss rates are illustrated as a function of the power-law index α in Figure 2 for different values of E_{\min} and E_{\max} . Here, we have normalized to a coronal luminosity of $L_X = 10^{30}$ erg s $^{-1}$ in the *GOES* 1–8 Å bandpass, which, for a fairly typical coronal temperature for the most active solar-like stars of 2×10^7 K, corresponds to $L_X \sim 3 \times 10^{30}$ erg s $^{-1}$ in the 0.2–2.5 keV and 0.5–10 keV bandpasses. This X-ray luminosity is that of a coronally saturated solar-like star with a ratio of X-ray to bolometric luminosity of $L_X/L_{\text{bol}} \sim 10^{-3}$, such as 47 Cas B or EK Dra (see, e.g., Telleschi et al. 2005).

For fiducial limits we have adopted $E_{\max} = 10^{34}$ erg and $E_{\min} = 10^{-6} E_{\max}$. The former corresponds to a reasonably large but fairly common flare on an active solar-type star. Figure 2 demonstrates that the particular choice of these integration limits is not important—changing the lower limit by a factor of 100, for example, barely affects the derived mass loss rate and changes the kinetic energy by an amount comparable to the uncertainty resulting from the power-law fit in Equation (2). The general conclusion from Figure 2 is that, for values of $\alpha \sim 2$ – 2.5 , the CME mass loss rate for a saturated solar-type star is $\dot{M} \sim 5 \times 10^{-10} M_{\odot} \text{ yr}^{-1}$. The corresponding CME

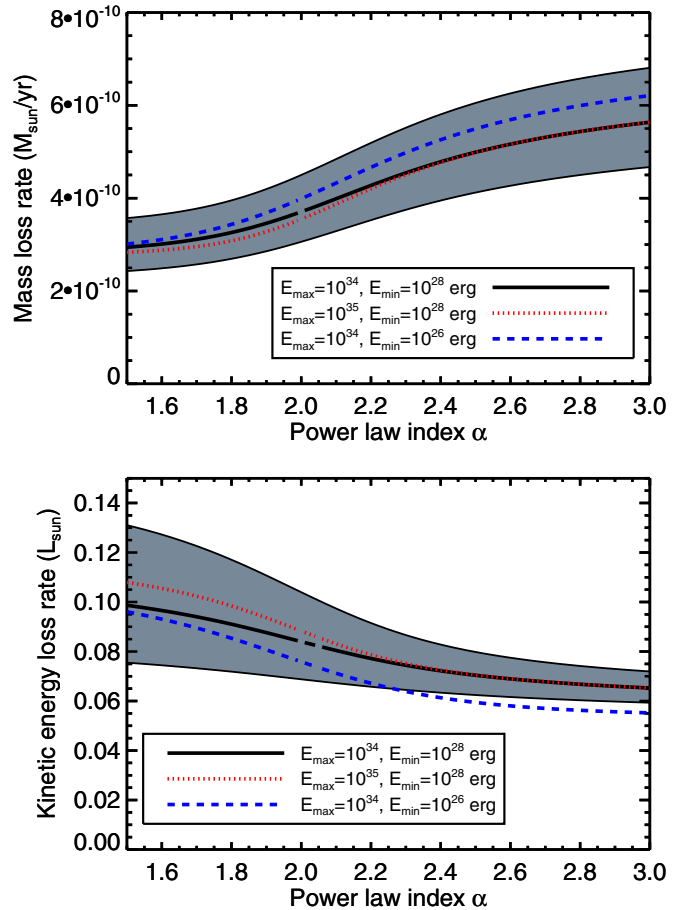


Figure 2. CME mass (top) and kinetic energy (bottom) loss rates vs. power-law index α for a 1–8 Å X-ray luminosity of $L_X = 10^{30}$ erg s $^{-1}$, according to Equations (8) and (9), respectively. Note that there are singularities corresponding to power-law indices $\alpha = 1 + \beta + \delta$ and $\alpha = 2$. The gray shaded areas represent the uncertainties in the loss rates corresponding to the uncertainties in the power-law fits in Equations (1) and (2).

(A color version of this figure is available in the online journal.)

kinetic energy requirement approaches $\dot{E}_{ke} \sim 0.1 L_{\odot}$. In the context of current ideas concerning mass loss and efficiency of magnetic energy dissipation on active late-type stars these values are extremely high and their implications are discussed in Sections 4.1 and 4.3.

The implied CME mass and energy loss rates in stars with magnetic activity significantly below the saturation threshold depend much more heavily on the X-ray bandpasses and the luminosity that enters the normalization factor in Equations (8) and (9). We use a relation between coronal temperature and 0.1–10 keV X-ray luminosity for solar-like stars based on those of Guedel et al. (1997) and Telleschi et al. (2005),

$$L_X = 6 \times 10^{25} \tilde{T}^{4.5} \text{ erg s}^{-1}, \quad (10)$$

where the constant and power-law index have been tailored slightly so as to represent the isothermal plasma temperature, \tilde{T} , that reproduces the observed hardness ratios ($L(1.0$ – $10 \text{ keV})/L(0.2$ – $1.0 \text{ keV})$) derived by Telleschi et al. (2005). The hard band adopted by those authors is similar to the *GOES* band (1.54–12.4 keV) and the relation in Equation (10) provides a reasonably accurate means for scaling the broadband X-ray luminosity to this harder bandpass. Model hardness ratios and bandpass conversion factors as a function of temperature were derived using the APEC radiative loss model,

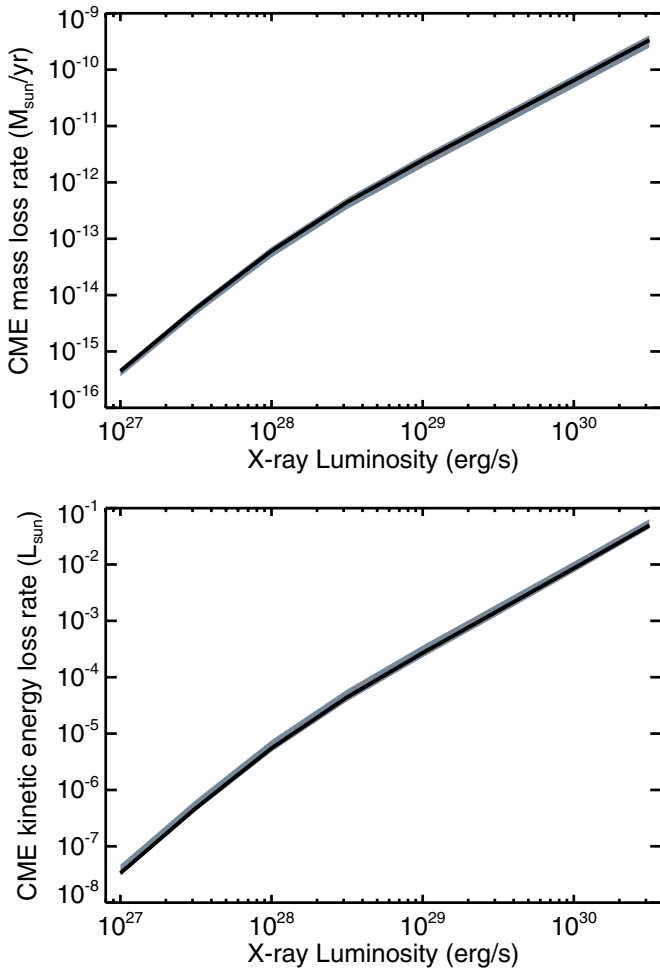


Figure 3. CME mass (top) and kinetic energy (bottom) loss rates vs. broadband X-ray luminosity. The solid curve represents the power-law index $\alpha = 2.25$. The gray shaded areas represent the range in the loss rates corresponding to the power-law index range $1.5 \leq \alpha \leq 3.0$.

(A color version of this figure is available in the online journal.)

as implemented in PIMMS.⁴ The resulting scaling factor depends approximately linearly on $\log L_X$, varying from ~ 0.3 at $L_X = 3 \times 10^{30} \text{ erg s}^{-1}$ to 10^{-3} at $L_X = 10^{27} \text{ erg s}^{-1}$.

Using the L_X to *GOES* bandpass scaling factor, we can obtain the CME mass and energy loss rates as a function of broadband X-ray luminosity. These are illustrated in Figure 3. Here, the minimum and maximum flare energies were assumed to be $E_{\min} = 10^{-6} E_{\max}$ and $E_{\max} = 10^4 L_X$, though again the results depend only weakly on the exact limits of integration. The CME mass loss rate as a function of X-ray luminosity can be approximated by a simple power law at higher energies and a polynomial over a larger energy range:

$$\log \dot{M}_c = -54.6 + 1.48 \log L_X; \quad L_X \geq 10^{28} \text{ erg s}^{-1}$$

$$\log \dot{M}_c = -1339 + 131 \log L_X - 4.37 \log^2 L_X + 0.049 \log^3 L_X, \quad (11)$$

where the latter third-order relation should be valid for L_X down to $10^{26} \text{ erg s}^{-1}$.

4. DISCUSSION

The reader familiar with the literature touched upon in Section 1 on winds from late-type main-sequence stars might

view the mass loss rates derived in Section 3 with incredulity. The CME kinetic energy loss rate approaching one-tenth of the stellar luminosity also seems implausibly high when compared with radiative losses through X-rays for saturated stars. For a range of spectral types this saturation level is consistently close to $10^{-3} L_{\text{bol}}$, with a scatter of a factor of 2–3 (e.g., Wright et al. 2011). The derivations themselves in Section 3 are, however, completely straightforward and the origin of the numbers is easy to understand simply through inspection of the solar CME data. At face value, uncertainties in the analysis resulting from the power-law fitting are also fairly small, resulting in mass and kinetic energy loss uncertainties of factors of a few. However, it should be kept in mind that there are relatively few CMEs at the higher energy and mass end of the observed distribution and systematic uncertainties resulting from this likely dominate.

4.1. Mass Loss

Also shown in Figure 1 is the vector corresponding to a constant ratio of mass loss to *GOES* X-ray energy loss converted to loss rates, $\dot{M} = 10^{-10}(L_X/10^{30}) M_{\odot} \text{ yr}^{-1}$, and the mean CME ejected mass versus flare X-ray fluence weighted by the CME–flare association fraction. For flare energies $\leq 3.5 \times 10^{29} \text{ erg}$, the latter lies remarkably parallel to the former (probably by coincidence, but if not it raises an interesting issue), and offset by a factor of five or so. One can see that this translates directly to the derived mass loss rate for a flare-dominated corona of a few $10^{-10} M_{\odot} \text{ yr}^{-1}$, as found in Section 3 and shown in Figure 2, with little dependence on the power-law index α .

The value of α essentially controls the weighting between flares of lower or higher energy. This is evident from Equation (5): for $\alpha < 2$, the X-ray luminosity tends to be dominated by the larger flares, whereas for $\alpha > 2$ smaller flares contribute the largest fraction to the observed emission. Since the flare association-weighted mean CME mass follows very closely a constant E versus mass, the total CME mass loss depends only weakly on α . Above the energy at which the CME–flare association is unity ($3.5 \times 10^{29} \text{ erg}$), the slope of the E –mass relation is more shallow and we expect the total derived mass loss to be lower for $\alpha < 2$, as is borne out in Figure 2.

It is of interest to see how the CME scaling might apply to solar levels of activity. From Figure 3, we find that, for a fairly active solar X-ray luminosity of $L_X \sim 10^{27} \text{ erg s}^{-1}$, the mass loss rate is $\dot{M}_c \sim 4 \times 10^{-16} M_{\odot} \text{ yr}^{-1}$ —a few percent of the total solar mass loss rate, in broad agreement with the average CME mass flux assessed by Vourlidis et al. (2010) between 1999 and 2003.

The conclusion from the mean E versus mass relation for solar flares and associated CMEs is that, if active stars are dominated by solar-like flares and we can extrapolate the relation in Figure 1 to higher flare energies, CME mass loss rates are very large—up to four orders of magnitude greater than the present-day solar wind and scaling with 1–8 Å band X-ray luminosity roughly according to $\dot{M} \sim 5 \times 10^{-10}(L_X/10^{30}) M_{\odot} \text{ yr}^{-1}$. Aarnio et al. (2012) find similar numbers for T Tauri stars (7×10^{-11} – $2 \times 10^{-9} M_{\odot} \text{ yr}^{-1}$) using a similar method to that employed here.

Can such high mass loss rates possibly be correct? For the most active stars, the CME energy requirements clearly pose a problem; we return to this in Section 4.3. In Section 1 we cited evidence that upper limits to wind-driven mass loss in active solar-type stars based on attempts to detect free–free radio emission were of the order of a few $10^{-11} M_{\odot} \text{ yr}^{-1}$ (Gaidos et al. 2000). This analysis assumed a spherically symmetric wind, but

⁴ <http://cxc.harvard.edu/toolkit/pimms.jsp>

a superposition of many CMEs should produce a qualitatively similar, though probably more clumpy and turbulent, outflow (see also Section 4.2). The most active star in the sample was π^1 UMa, with $\dot{M} \leq 5 \times 10^{-11} M_{\odot} \text{ yr}^{-1}$. This star has a broadband X-ray luminosity of $L_X \sim 10^{29} \text{ erg s}^{-1}$ (Drake et al. 1994; Telleschi et al. 2005)—an order of magnitude or so below the saturation level. Based on our \dot{M}_c versus L_X relation in Figure 3, this implies $\dot{M} \sim 3 \times 10^{-12} M_{\odot} \text{ yr}^{-1}$ —well within the (Gaidos et al. 2000) upper limit. This is also consistent with the maximum allowed mass loss rate of $\leq 10^{-11} M_{\odot}$ for a 10^7 K “wind” estimated by Lim & White (1996) based on the requirement of radio transparency consistent with radio detections of active stars.

Wood et al. (2002, 2005) estimated mass loss rates for a handful of stars of different activity level using astrospheric Ly α absorption. While their analysis assumed a spherically symmetric outflow with a wind speed of 400 km s^{-1} , we would again expect a similar observational signature from a superposition of CMEs. The Wood et al. measurements scale with wind ram pressure, so an outflow comprised of generally faster CMEs would imply a proportionately lower mass loss rate. The mass-weighted mean CME speed in the Yashiro & Gopalswamy (2009) sample is 1015 km s^{-1} , implying a lower mass loss by only a factor of ~ 2 . For a small sample of G and K dwarfs, Wood et al. (2005) found $\dot{M} \propto F_X^{1.34 \pm 0.18}$, where F_X is the surface X-ray flux. This is similar to the CME mass loss power-law relation we found in Equation (11). While they caution against extrapolating the relation to higher activity levels, scaling to the X-ray surface flux for a solar-like star corresponding to $L_X = 3 \times 10^{30}$ yields $\dot{M} \sim 10^{-10} M_{\odot} \text{ yr}^{-1}$, only a factor of a few lower than our CME-based estimate. At a flux level of π^1 UMa, the relation corresponds to $\dot{M} \sim 10^{-11} M_{\odot} \text{ yr}^{-1}$ —again similar to the CME scaling since the power-law relations are also very similar.

The scaling of the solar wind to higher magnetic activity levels remains a very uncertain endeavor owing to the lack of a comprehensive theory explaining the solar wind itself. Cohen (2011) argues that scaling mass loss according to X-ray luminosity is misleading because the latter is dictated by the closed magnetic field, while the former is dominated by open flux. He argues that mass loss rates are unlikely to exceed $10^{-12} M_{\odot} \text{ yr}^{-1}$. The model of Cranmer & Saar (2011) is driven by the energy flux of magnetohydrodynamic turbulence from the convection zone and the filling factor of open field. Their mass loss rate for a saturated solar-like star is a few $10^{-12} M_{\odot} \text{ yr}^{-1}$, which is two orders of magnitude lower than the direct CME scaling. This suggests that the indirect wind observations of Wood et al. could in fact be observations of quasi-continuous CME mass loss for the more active stars of the sample, rather than a direct analogy to the solar wind.

Taken at face value, the solar CME data, combined with currently scant data on stellar winds and models of wind mass loss, suggest that at the highest activity levels mass loss could be dominated by CMEs, with a gradual transition to wind-dominated mass loss toward lower activities. In the context of the study of Cohen (2011), unlike a steady wind, CME mass loss is expected to scale with X-ray luminosity because flares and CMEs generally originate from active regions that are dominated by closed field.

In the context of the mass budget for individual CMEs, Equation (1) implies that for stellar flares with a total 1–8 Å flare X-ray fluence of 10^{34} erg , the mean ejected mass is about $4 \times 10^{18} \text{ g}$. If the CME source plasma resides in the corona, this

mass is uncomfortably large. It corresponds to the entire mass of a corona with a scale height of $0.1 R_{\odot}$, an emission measure of a few 10^{52} cm^{-3} (like that of 47 Cas B from analysis of Telleschi et al. 2005) and a quiescent active region-like density of 10^{10} cm^{-3} . A fluence of 10^{34} erg , even limited to the 1–8 Å GOES band, is still quite a modest flare compared with the largest flares seen on the most active stars and on T Tauri stars, whose broadband X-ray fluences can reach 10^{37} erg (e.g., Schrijver et al. 2012). This corresponds to $\sim 3 \times 10^{36} \text{ erg}$ in the 1–8 Å band based on the scaling derived in Section 3, and would imply a mean ejected mass a factor of 30 higher still. These large mass requirements suggest that the solar CME X-ray fluence–mass relation must break toward the largest flares.

4.2. Early Faint Sun Paradox

Could the mass loss through CMEs on an early active Sun be relevant to the “early faint Sun paradox”? Sagan & Mullen (1972) pointed out that the lower solar luminosity predicted by stellar evolutionary theory earlier in the history of the solar system implies that for contemporary albedos and atmospheric composition global mean temperatures would have been below the freezing point of seawater until about 2.3 Gyr ago, in contradiction with geological evidence for liquid oceans. Possible solutions to this paradox include higher concentrations of greenhouse gases and aerosols (e.g., Sagan & Mullen 1972; Kasting 1993), a lower global albedo, either through less cloud coverage (e.g., Shaviv 2003) or a smaller continental land mass (Rosing et al. 2010). An alternative solution is an early Sun more massive by several percent that has since been whittled down by mass loss (e.g., Guzik et al. 1987; Sackmann & Boothroyd 2003; Minton & Malhotra 2007).

Wood et al. (2002) note that their inferred steady wind mass loss rates are insufficient when combined with relations for the secular decline of X-ray surface flux: the cumulative mass loss from an age of 1 Gyr or so is much less than 1%. As noted in Section 4.1, we find a relation between mass loss from CMEs and X-ray flux consistent with the observed steady wind relation of Wood et al. (2002)— $\dot{M} \propto L_X^{1.5}$ for active stars, compared with their $\propto F_X^{1.34 \pm 0.18}$. For a solar-like star such as κ^1 Cet with an age of about 0.75 Gyr and $L_X \sim 10^{29} \text{ erg s}^{-1}$, the mass loss rate is similar to that of π^1 UMa considered in Section 4.1, $\dot{M} \sim 3 \times 10^{-12} M_{\odot} \text{ yr}^{-1}$. Even if such a rate lasted for over a Gyr, it would amount to less than $0.01 M_{\odot}$, or an order of magnitude less than required to resolve the early faint Sun paradox unilaterally.

4.3. Energy Loss, Dynamo Saturation, and CME Implications

A key question begging from the beginning of Section 4 is what fraction of the stellar bolometric luminosity can be scavenged by magnetic processes that give rise to flares and CMEs? Saturation of magnetic activity for the most active stars pegs broadband X-ray radiative losses at $\sim 10^{-3} L_{\text{bol}}$, which has generally been used as a saturation energy dissipation rate for convection zone dynamos. However, X-rays represent only one aspect of the energy budget of solar flares. The total radiative and non-thermal energy can be factors of 10–100 higher than the GOES 1–8 Å fluence, and possibly as much as associated CME kinetic energies (e.g., Woods et al. 2004; Emslie et al. 2005; Raymond 2008; Kretzschmar et al. 2010; Kretzschmar 2011). This translates to factors of ~ 3 –30 higher than broadband X-ray fluence for flare-like temperatures. If active stellar coronae are dominated by flares and their behavior is similar on active stars,

then energy requirements of flares alone could amount to 1% or more of the bolometric luminosity.

We found in Section 3 that scaling solar CME kinetic energy to a flare-dominated corona at saturated activity level would require a staggering fraction of the stellar luminosity, approaching 10%. If we declare 10% of L_{bol} too high a fraction of the total stellar energy budget to expend on CMEs, the implication is that the solar CME data *cannot* be extrapolated to significantly higher energies in the way we have done in Section 3. Both CME speed and mass increase with X-ray fluence in the Yashiro & Gopalswamy (2009) sample. To avoid energy budget problems, either the CME kinetic energy versus X-ray fluence must flatten out toward higher flare energies, implying that CME speed, mass, or both flatten out, or the CME–flare association rate must drop back significantly below 1. It is commonly argued that flares without associated CMEs are confined by overlying magnetic field (e.g., Svestka & Cliver 1992). Active regions on active stars could confine more energetic CMEs associated with stronger flares because of stronger magnetic fields or different magnetic topology.

A fit to the mean CME speed, analogous to those in Equations (1) and (2), finds $v_c(E) = 3.6 \times 10^{-4} E^{0.22} \text{ km s}^{-1}$, and for the same 10^{34} erg flare fluence corresponds to $11,000 \text{ km s}^{-1}$. The highest speed in the CME sample of Yashiro & Gopalswamy (2009) is about 3000 km s^{-1} . The kinetic energy problem would be largely resolved were the ejection velocity to level out at this value toward higher flare energies.

The kinetic energy problem for very large CMEs is possibly related to the observed cutoff in solar energetic particle (SEP) fluence for particle energies above 10 MeV first inferred from cosmogenic radionuclides by Lingenfelter & Hudson (1980; see also Reedy 1996; Hudson 2007; Schrijver et al. 2012; Usoskin & Kovaltsov 2012). The SEP fluence frequency spectrum breaks at approximately 10^{10} cm^{-2} . Several different explanations have been suggested for this, such as an event energy dependence of SEP spectral distributions, particle propagation effects in the heliosphere, or SEP opening angles depending on the energy of the triggering event (e.g., Schrijver et al. 2012). Hudson (2007) notes that the SEP cutoff energy corresponds approximately to flares of X10 class (peak *GOES* 1–8 Å flux of 10^{-3} W m^{-2} or $3 \times 10^{27} \text{ erg s}^{-1}$). He argues that there appears to be no corresponding cutoff in the frequency of such flares, and any steeping of the flare frequency spectrum must happen at significantly higher energies. This suggests there might be another limiting factor governing SEP production. Since SEPs are thought to be largely accelerated in CME-driven coronal and interplanetary shocks (e.g., Kahler et al. 1978; Reames 1999; Gopalswamy et al. 2002; Cliver et al. 2004), a cutoff in energy could result from a corresponding limit to CME velocity or kinetic energy. How such a constraint might translate to significantly more active stars would then be important for the CME kinetic energy budget: whether it scales with maximum flare, or active region, available energy, or is a more fundamental physical limitation with a cutoff at the same energy as seen on the Sun.

We tentatively conclude that the relation between both CME mass and speed with flare fluence must flatten toward larger flare energies. This behavior would appear to differ to the scaling of magnetic flux and flare properties from solar to active stellar cases. Pevtsov et al. (2003) find that, instead, the relationship between unsigned magnetic flux and X-ray spectral radiance for different regions of the Sun scales over 12 orders of magnitude to active stars. Flare temperatures, emission measures, and hard

versus soft components also appear to show a similar scaling from solar flares all the way to giant flares on active stars (Feldman et al. 1995; Isola et al. 2007; Aschwanden et al. 2008). Solar CME energies are limited by the free energy available in solar active regions, which Gopalswamy et al. (2010) note is $<10^{36}$ erg and usually at most 10^{33} – 10^{34} erg (e.g., Emslie et al. 2012; Aulanier et al. 2013); in this context it would be of interest to assess the energy available in stellar active regions, which might be possible through Zeeman–Doppler imaging magnetograms.

The large “hidden” CME and flare energy requirements of a corona whose X-ray emission is dominated by flares implies that stars at the X-ray activity saturation threshold are extracting much more than $10^{-3} L_{\text{bol}}$ of energy, probably by an order of magnitude or more. This suggests that saturated stars are experiencing a magnetic energy dissipation limit, rather than a limit imposed by the ability of the star to sustain X-ray emitting loops due to centrifugal stripping or poleward migration of magnetic flux (Stępień et al. 2001; Jardine & Unruh 1999; Wright et al. 2011). That is, the maximum amount of the total energy budget able to be extracted by a magnetic dynamo has been reached. If we allow CMEs to consume 1% of the stellar energy budget on X-ray saturated stars, the implied mass loss for saturated stars is $\dot{M}_c \sim 5 \times 10^{-11} M_{\odot} \text{ yr}^{-1}$.

5. CONCLUSIONS

Mean solar CME mass and kinetic energy are related to the associated flare X-ray fluence by power laws. If active stellar coronal X-ray emission is comprised of flares as observations suggest, and these flares adhere to the observed solar flare–CME scalings found here, very high CME mass loss rates exceeding $10^{-10} M_{\odot}$ are implied for the most active stars, consuming a tenth of the stellar bolometric luminosity. Since this energy requirement seems too high, we conclude that solar flare–CME relations cannot be extrapolated to arbitrarily high flare energies: CME mass and/or kinetic energy versus flare X-ray fluence must flatten off at flare energies $\gtrsim 10^{31}$ erg. A more reasonable CME energy budget of 1% of L_{bol} implies $\dot{M}_c \sim 5 \times 10^{-11} M_{\odot}$. Even for budgets an order of magnitude lower it seems likely that mass loss from active stars will be dominated by CMEs. The large “hidden” energy budget of flares and associated CMEs raises the question of what is the maximum amount of energy a solar-like star can extract from a magnetic dynamo? If saturated stars are dominated by flares, this energy is likely to be an order of magnitude larger than the observed broadband X-ray saturation level of $10^{-3} L_{\text{bol}}$.

J.J.D. was funded by NASA contract NAS8-03060 to the Chandra X-Ray Center (CXC) and thanks the CXC director, H. Tananbaum, and the CXC science team for continuing advice and support. O.C. was supported by *Chandra* Grant TM2-13001X. J.J.D. also thanks David Soderblom for organizing a workshop on the Faint Early Sun that provided the impetus for this study, and Vinay Kashyap for fruitful discussion. Finally, we thank the referee for a very helpful report that enabled us to improve the manuscript significantly.

REFERENCES

- Aarnio, A. N., Matt, S. P., & Stassun, K. G. 2012, *ApJ*, **760**, 9
 Aarnio, A. N., Stassun, K. G., Hughes, W. J., & McGregor, S. L. 2011, *SoPh*, **268**, 195
 Andrews, M. D. 2003, *SoPh*, **218**, 261

- Aschwanden, M. J., Stern, R. A., & Güdel, M. 2008, *ApJ*, **672**, 659
- Audard, M., Güdel, M., Drake, J. J., & Kashyap, V. L. 2000, *ApJ*, **541**, 396
- Aulanier, G., Démoulin, P., Schrijver, C. J., et al. 2013, *A&A*, **549**, A66
- Bai, T. 1993, *ApJ*, **404**, 805
- Caramazza, M., Flaccomio, E., Micela, G., et al. 2007, *A&A*, **471**, 645
- Cliver, E. W., Kahler, S. W., & Reames, D. V. 2004, *ApJ*, **605**, 902
- Cohen, O. 2011, *MNRAS*, **417**, 2592
- Collura, A., Pasquini, L., & Schmitt, J. H. M. 1988, *A&A*, **205**, 197
- Cranmer, S. R., & Saar, S. H. 2011, *ApJ*, **741**, 54
- Datlowe, D. W., Elcan, M. J., & Hudson, H. S. 1974, *SoPh*, **39**, 155
- Drake, J. F. 1971, *SoPh*, **16**, 152
- Drake, J. J., Peres, G., Orlando, S., Laming, J. M., & Maggio, A. 2000, *ApJ*, **545**, 1074
- Drake, S. A., Singh, K. P., White, N. E., & Simon, T. 1994, *ApJL*, **436**, L87
- Emslie, A. G., Dennis, B. R., Holman, G. D., & Hudson, H. S. 2005, *JGRA*, **110**, 11103
- Emslie, A. G., Dennis, B. R., Shih, A. Y., et al. 2012, *ApJ*, **759**, 71
- Feldman, U., Laming, J. M., & Doschek, G. A. 1995, *ApJL*, **451**, L79
- Gaidos, E. J., Güdel, M., & Blake, G. A. 2000, *GeoRL*, **27**, 501
- Gopalswamy, N., Akiyama, S., Yashiro, S., & Mäkelä, P. 2010, in *Magnetic Coupling between the Interior and Atmosphere of the Sun*, ed. S. S. Hasan & R. J. Rutten (Berlin: Springer), 289
- Gopalswamy, N., Yashiro, S., Michalek, G., et al. 2002, *ApJL*, **572**, L103
- Güdel, M., Arzner, K., Audard, M., & Mewe, R. 2003, *A&A*, **403**, 155
- Guedel, M. 1997, *ApJL*, **480**, L121
- Guedel, M., Guinan, E. F., & Skinner, S. L. 1997, *ApJ*, **483**, 947
- Guzik, J. A., Willson, L. A., & Brunish, W. M. 1987, *ApJ*, **319**, 957
- Hannah, I. G., Hudson, H. S., Battaglia, M., et al. 2011, *SSRv*, **159**, 263
- Hudson, H. S. 1991, *SoPh*, **133**, 357
- Hudson, H. S. 2007, *ApJL*, **663**, L45
- Isola, C., Favata, F., Micela, G., & Hudson, H. S. 2007, *A&A*, **472**, 261
- Jardine, M., & Unruh, Y. C. 1999, *A&A*, **346**, 883
- Kahler, S. W., Hildner, E., & Van Hollebeke, M. A. I. 1978, *SoPh*, **57**, 429
- Kashyap, V. L., Drake, J. J., Güdel, M., & Audard, M. 2002, *ApJ*, **580**, 1118
- Kasting, J. F. 1993, *Natur*, **364**, 759
- Kawaler, S. D. 1988, *ApJ*, **333**, 236
- Khodachenko, M. L., Lammer, H., Lichtenegger, H. I. M., et al. 2007a, *P&SS*, **55**, 631
- Khodachenko, M. L., Ribas, I., Lammer, H., et al. 2007b, *AsBio*, **7**, 167
- Kretzschmar, M. 2011, *A&A*, **530**, A84
- Kretzschmar, M., de Wit, T. D., Schmutz, W., et al. 2010, *NatPh*, **6**, 690
- Krucker, S., & Benz, A. O. 1998, *ApJL*, **501**, L213
- Lammer, H., Lichtenegger, H. I. M., Kulikov, Y. N., et al. 2007, *AsBio*, **7**, 185
- Lim, J., & White, S. M. 1996, *ApJL*, **462**, L91
- Lin, R. P., Schwartz, R. A., Kane, S. R., Pelling, R. M., & Hurley, K. C. 1984, *ApJ*, **283**, 421
- Lingenfelter, R. E., & Hudson, H. S. 1980, in *The Ancient Sun: Fossil Record in the Earth, Moon and Meteorites*, ed. R. O. Pepin, J. A. Eddy, & R. B. Merrill (Oxford: Pergamon), 69
- Maehara, H., Shibayama, T., Notsu, S., et al. 2012, *Natur*, **485**, 478
- Matt, S., & Pudritz, R. E. 2008, *ApJ*, **678**, 1109
- Minton, D. A., & Malhotra, R. 2007, *ApJ*, **660**, 1700
- Pallavicini, R., Golub, L., Rosner, R., et al. 1981, *ApJ*, **248**, 279
- Pevtsov, A. A., Fisher, G. H., Acton, L. W., et al. 2003, *ApJ*, **598**, 1387
- Porter, J. G., Fontenla, J. M., & Simnett, G. M. 1995, *ApJ*, **438**, 472
- Preusse, S., Kopp, A., Büchner, J., & Motschmann, U. 2005, *A&A*, **434**, 1191
- Raymond, J. C. 2008, *JApA*, **29**, 187
- Reames, D. V. 1999, *ApJ*, **518**, 473
- Reedy, R. C. 1996, in *ASP Conf. Ser. 95, Solar Drivers of the Interplanetary and Terrestrial Disturbances*, ed. K. S. Balasubramaniam, S. L. Keil, & R. N. Smartt (San Francisco, CA: ASP), 429
- Reiners, A., & Mohanty, S. 2012, *ApJ*, **746**, 43
- Rosing, M. T., Bird, D. K., Sleep, N. H., & Bjerrum, C. J. 2010, *Natur*, **464**, 744
- Rubin, D. B. 1996, *Am. Stat. Assoc.*, **91**, 473
- Sackmann, I.-J., & Boothroyd, A. I. 2003, *ApJ*, **583**, 1024
- Sagan, C., & Mullen, G. 1972, *Sci*, **177**, 52
- Schrijver, C. J., Beer, J., Baltensperger, U., et al. 2012, *JGRA*, **117**, 8103
- Shaviv, N. J. 2003, *JGRA*, **108**, 1437
- Stauffer, J. B., & Hartmann, L. W. 1986, *PASP*, **98**, 1233
- Stelzer, B., Flaccomio, E., Briggs, K., et al. 2007, *A&A*, **468**, 463
- Stępień, K., Schmitt, J. H. M. M., & Voges, W. 2001, *A&A*, **370**, 157
- Svestka, Z., & Cliver, E. W. 1992, in *IAU Colloq. 133, Eruptive Solar Flares*, ed. Z. Svestka, B. V. Jackson, & M. E. Machado (Lecture Notes in Physics, Vol. 399; Berlin: Springer), 1
- Telleschi, A., Güdel, M., Briggs, K., et al. 2005, *ApJ*, **622**, 653
- Usoskin, I. G., & Kovaltsov, G. A. 2012, *ApJ*, **757**, 92
- Vourlidas, A., Howard, R. A., Esfandiari, E., et al. 2010, *ApJ*, **722**, 1522
- Weber, E. J., & Davis, L., Jr. 1967, *ApJ*, **148**, 217
- Wood, B. E., Müller, H., Zank, G. P., & Linsky, J. L. 2002, *ApJ*, **574**, 412
- Wood, B. E., Müller, H.-R., Zank, G. P., Linsky, J. L., & Redfield, S. 2005, *ApJL*, **628**, L143
- Woods, T. N., Eparvier, F. G., Fontenla, J., et al. 2004, *GeoRL*, **31**, 10802
- Wright, N. J., Drake, J. J., Mamajek, E. E., & Henry, G. W. 2011, *ApJ*, **743**, 48
- Yashiro, S., & Gopalswamy, N. 2009, in *IAU Symp. 257, Universal Heliophysical Processes*, ed. N. Gopalswamy & D. F. Webb (Cambridge: Cambridge Univ. Press), 233